In Vivo Trabecular Bone Morphologic and Mechanical Relationship Using High-Resolution 3-T MRI

Angel Alberich-Bayarri[1]
Luis Marti-Bonmati[1]
Roberto Sanz-Requena[1]
Elena Belloch[1]
David Moratal[2]

OBJECTIVE. The purpose of this study was to investigate the in vivo morphologic and elastic parameters of trabecular bone with high-resolution 3-T MRI in a healthy reference population.

SUBJECTS AND METHODS. A series of wrist MR images were acquired with high-spatial-resolution (180 μm) isotropic voxels from 40 subjects without reported bone disease. After image postprocessing, the bone volume-to-total volume ratio, trabecular thickness, trabecular separation, and trabecular number were calculated in the morphologic analysis. Trabecular bone was mechanically simulated using the finite-element method to calculate the apparent elastic modulus parameter. The relationship between morphologic and mechanical parameters was studied. The influence of the analyzed bone volume was also investigated.

RESULTS. Statistically significant sex influences were found on the bone volume-to-total volume ratio ($p = 0.003$), trabecular thickness ($p = 0.02$), and apparent elastic modulus ($p = 0.01$); these parameters were lower in women. However, trends were found only on trabecular separation ($p = 0.06$) and trabecular number ($p = 0.07$). Age had no statistically significant influence in any morphologic (bone volume-to-total volume ratio, $r = -0.24$, $p = 0.13$; trabecular thickness, $r = -0.03$, $p = 0.88$; trabecular separation, $r = 0.12$, $p = 0.47$; and trabecular number, $r = -0.23$, $p = 0.16$) or elastic (apparent elastic modulus, $r = -0.18$, $p = 0.26$) parameter. A statistically significant relationship between apparent elastic modulus and the square of bone volume-to-total volume ratio was found ($r = 0.968$, $p < 0.001$). This association was not seen ($r = 0.185$, $p = 0.25$) and apparent elastic modulus results were considerably different ($p < 0.001$) if the volume of analyzed bone was reduced.

CONCLUSION. We found that bone volume-to-total volume ratio, trabecular thickness, and apparent elastic modulus are parameters significantly influenced by sex. Apparent elastic modulus results show a relationship with bone volume-to-total volume ratio. Trabecular bone volume should be maximized for an appropriate mechanical analysis.

Keywords: elastic modulus, finite element, MRI, osteoporosis, trabecular bone

DOI:10.2214/AJR.07.3528

Received December 10, 2007; accepted after revision April 13, 2008.

Study partially supported by the Sociedad Española de Radiología Médica through the SERAM-Industria 2005 grant.

D. Moratal partially supported by the Vicerectorat d'Innovació i Desenvolupament of the Universitat Politècnica de València (PAID-06-07 / 3104).

[1]Department of Radiology, Hospital Quirón, Avda. Blasco Ibáñez, 14, 46010 Valencia, Spain. Address correspondence to A. Alberich-Bayarri (aalberich.val@quiron.es).

[2]Electronics Engineering Department, Universidad Politècnica de València, Valencia, Spain.

AJR 2008; 191:721–726

0361–803X/08/1913–721

High-resolution MRI can be used in the postprocessing and quantification of different parameters that may act as disease biomarkers. High spatial resolution in a reasonable acquisition time can be achieved with the increased signal-to-noise ratio of the 3-T MR scanners. Regarding bone evaluation, these images can give information of the trabecular cancellous structure with great detail.

The diagnosis of osteoporosis is based on the quantification of bone mineral density (BMD) by dual energy x-ray absorptiometry (DEXA) techniques. Because osteoporosis affects not only the BMD but also the trabecular bone microarchitecture [1], BMD is not sufficiently comprehensive for complete characterization of trabecular bone deterioration [2]. The architectural abnormalities associated with osteoporosis produce an alteration of specific structural organization and mechanical parameters of cancellous bone.

With the aim of quantifying trabecular bone characteristics, advanced image postprocessing techniques with morphologic and mechanical elastic analysis can be applied to series of axial 3D MR images of the wrist to evaluate both morphology and mechanical bone properties in healthy subjects. Because trabecular thinning and pore size increment are clear biomarkers of osteoporosis [3], it seems quite relevant to develop a structural characterization of trabecular bone on the basis of morphologic parameters. The most relevant morphologic values in the characterization of trabecular bone are the bone volume-to-total volume ratio, trabecular

thickness, trabecular separation, and trabecular number.

On the other hand, microarchitecture deterioration induced by osteoporosis supposes an increase in the fracture risk due to trabeculae disorganization. Any approach to the quantification of trabecular bone microstructure elasticity degree should be considered to evaluate the fracture risk. Different material properties related to the stress–strain relationship, such as elasticity, can be evaluated by the quantification of the apparent elastic modulus (also called apparent Young's modulus) parameter.

Structural simulations are currently being developed in biomedical engineering by application of the finite element (FE) method, which consists of the division of a continuum into discrete elements that define a linear system of equations with displacements and forces to be solved. A study of the mechanical properties of the trabecular bone can be obtained by the application of the FE method to the trabecular bone voxel-meshed structures [4]. Trabecular bone reconstructions can be simulated under compression to obtain stresses, strains, and displacements of each element in the cancellous bone discrete model. Processing of these mechanical solutions can be implemented by the direct application of the homogenization theory to estimate the apparent elastic modulus of the whole trabecular bone model.

Our objective was to characterize the architectural structure of cancellous bone in healthy subjects to obtain reference morphologic and elastic parameters to define their values and the relationships between them. This knowledge may be useful if these properties are finally determined to be bone disease biomarkers.

Subjects and Methods

Subjects

To be included, subjects did not have to present any history of bone disease, traumatic injury to the wrist, or metabolic abnormality. All MRI acquisitions were evaluated by radiologists. Ultimately, 40 subjects with nonsignificant wrist irregularities were selected for the study. The clinical reason for the MR examinations was to rule out articular wrist ligamentous abnormalities associated with pain. Because the examinations were performed as clinical tests, no specific informed consent was obtained for the trabecular analysis. There were 21 women and 19 men, with an age ranging from 18 to 80 years (mean [± SD] 38 ± 15 years). Both sexes were comparable regarding age ($p = 0.08$, Student's t test; 34 ± 9 vs 42 ± 18 years for men and women, respectively).

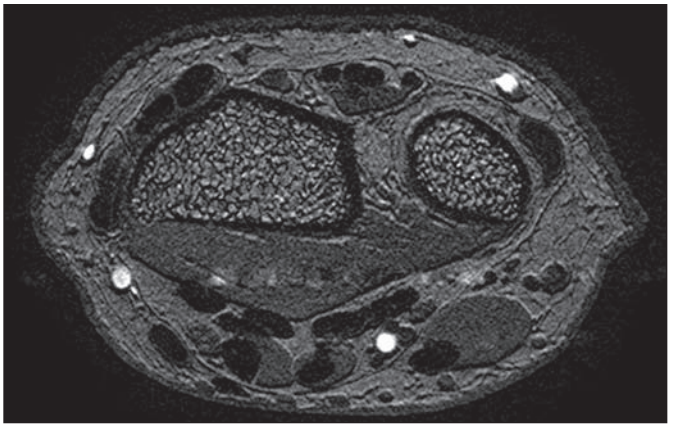

Fig. 1—Example of axial MR image acquired for trabecular bone characterization in 24-year-old healthy man. Acquired isotropic spatial resolution of 180 μm × 180 μm × 180 μm is achieved.

Image Acquisition

All images were acquired using a 3-T MR scanner (Achieva, Philips Healthcare) using a surface phased-array wrist coil with four channels. The MR sequence was a 3D spoiled T1-weighted gradient-echo (TR/TE, 56/5; flip angle, 25°) with an acquired matrix of 512 × 512 and 59 transverse partitions. The acquisition time was 5 minutes 42 seconds. The geometric parameters (slice thickness and pixel size) were chosen to obtain a spatial resolution of 180 × 180 × 180 μm, with the highest signal-to-noise ratio (SNR) and contrast between bone and marrow. Axial images were obtained from the distal metaphysis of the radius (Fig. 1).

Three-Dimensional Reconstruction of the Trabeculae

Processing algorithms were implemented in Matlab R2007a software (The MathWorks). An initial segmentation of the trabecular region in each slice was developed with an automated location of the radial cortex. The key of the method lies in the observation of two adjacent slices: Cortical bone conserves its shape, whereas intensities corresponding to the bone marrow are different from each other. Using this property, automated segmentation was performed by contour-fitting techniques on the basis of snakes (adaptive contour fitting technique) [5, 6]. The initial contour needed to start the segmentation algorithm was obtained by the application of image filters followed by pixel binarization. Each calculated contour was used as the initial condition for the adjacent slice.

Once the trabecular bone region was isolated, the bone volume fraction (BVF) map was calculated after discriminating voxels of pure marrow from those partially occupied by bone. Small signal intensity heterogeneities associated with the use of surface coils were statistically corrected by determining the local threshold intensities. Afterward, this local threshold was used to classify pixels into bone or marrow, performing the image equalization [7].

Because the true trabecula dimension (approximately 80–150 μm) is smaller than the acquired pixel size (180 μm), images were processed to virtually increase the spatial resolution, remove the trabecular blur, and minimize partial volume effects. Subvoxel processing was applied [8], finally obtaining voxels of 90 × 90 × 180 μm. Complete discrimination between bone and marrow voxels was achieved after thresholding binarization in each image set with the Otsu's method [9]. Finally, a logical 3D reconstruction of the whole cancellous structure was obtained (Fig. 2).

Morphologic Analysis

A structural analysis of the 3D structure was developed to characterize the morphologic parameters of the cancellous bone. All these algorithms were also implemented in Matlab R2007a

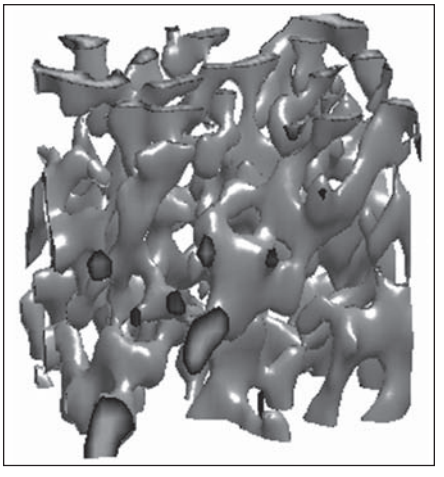

Fig. 2— Rendered 3D reconstruction of small portion of the trabecular bone in 31-year-old healthy man provides better observation of details.

to estimate the main morphologic parameters of bone volume-to-total volume ratio, trabecular thickness, trabecular separation, and trabecular number. To represent the percentage of bone voxels in the whole segmented volume, bone volume-to-total volume ratio was calculated by dividing the number of bone voxels of the 3D reconstruction by the global number of elements.

The trabecular thickness represents the mean thickness value of all the beams of trabecular bone of the 3D structure, measured in each slice and then averaged for all the slices of the 3D structure. First, a 2D skeletonization algorithm was applied and pixels labeled as trabeculae axis selected. Pixels corresponding to the boundary of the trabeculae were also detected by the application of a contour-detection algorithm. Then, the distance-transform method [10] was applied to the contour image to obtain the minimum distance from each pixel to the contour. The skeletonized image was multiplied by the result of the transform distance to obtain the minimum distance from each pixel of the skeleton or center line of the trabecular bone rod to the boundary—that is, the half value of the trabecular thickness.

The mean size of the intertrabecular spaces or pores defined the trabecular separation and was determined by calculating the mean number of contiguous voxels occupied by marrow in each one of the three space directions. The trabecular number, which gives an idea of the percentage of trabecular bone present in the volume against the mean trabecular thickness, was calculated by dividing the bone volume-to-total volume ratio by the trabecular thickness [11].

Mechanical Analysis

Trabecular bone was mechanically tested under simulation using the obtained 3D trabecular reconstructions. The FE method was applied on cubic samples of trabecular bone reconstruction of large dimensions (1.5 × 2 × 1 cm; total, 3 cm^3) to simulate a static uniaxial compression stress–strain test, with a total computation time of approximately 4 hours (PC with an Intel Core 2 Duo processor at 1.86 GHz and 1 GB of RAM).

The FE meshes were built by direct conversion from the 3D reconstruction voxels to eight-noded isotropic hexahedron (brick) elements (Fig. 3) (Saxena R, et al., presented at the 1999 annual Northeast Bioengineering Conference of the IEEE) using a self-developed fast-mesher algorithm. Each element was set to have compact bone material properties (Young's modulus, E = 10 GPa; Poisson's ratio, σ = 0.3) [12, 13]. In the simulation, null displacement was imposed on nodes from one side whereas a deformation (ε) of 10% of the edge length was specified on nodes from the opposite side to simulate compression.

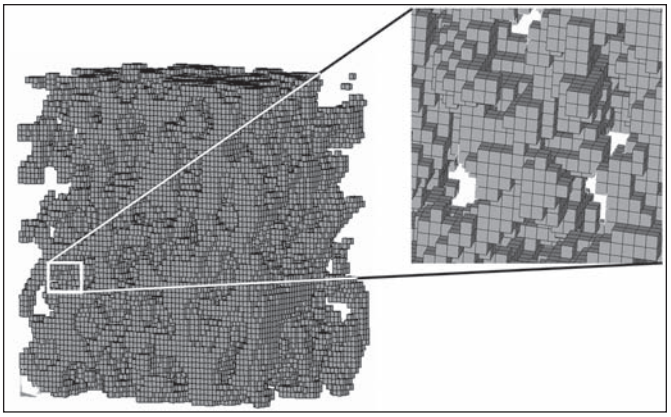

Fig. 3— Finite element mesh of large-volume trabecular bone reconstruction in 36-year-old healthy woman based on hexahedron or brick elements. Zoomed region shows detail of brick elements piled up and compounding structure.

The solution of the FE linear system of equations was calculated using Ansys, version 10.0 software (Ansys). Results of nodal displacements of the structure, nodal stresses and strains, and reaction forces were obtained in the solution of the FE method [14]. Moreover, an elastic characterization of the whole structure was performed by application of the homogenization theory [15, 16]. Results of the FE solution were processed to obtain the apparent elastic modulus parameter of the trabecular bone sample.

Reaction forces on nodes (F_n) from the fixed side were processed to obtain the apparent elastic modulus value (E_{app}) of the specimen by

$$E_{app} = \frac{1}{\varepsilon A}\sum_n F_n$$

where the modulus expressed the fraction of the total sum value of the nodal reactions of the fixed side by the area A of that side [16]. The obtained value was then divided by the global deformation suffered by the sample ε and, finally, E_{app} was calculated for the whole 3D structure.

Relationship Between Morphologic and Mechanical Parameters

The morphology–elasticity relationships for estimation of elastic properties of human trabecular bone were also assessed. The relationship between apparent elastic modulus and bone volume-to-total volume ratio [17, 18] was calculated to validate our apparent elastic modulus measurements and further characterize cancellous bone properties.

Influence of Analyzed Volume

With the aim of reducing the computational burden and to save time, an evaluation of the influence of the 3D sample size in the reliability of the measurements and the relationship between morphologic and mechanical parameters was also calculated. Therefore, simulations were also applied to a volume with reduced dimensions (0.5 × 0.5 × 1 cm; total, 0.25 cm^3), with a total computation time of approximately 20 minutes (91.6% decrease).

Statistical Analysis

Normal data distribution was checked by the application of the Kolmogorov-Smirnov test. Mean values were compared between men and women using the Student's t test distribution for independent samples with Levene's test for the equality of variances. The limit of significance was set at $p < 0.05$. The relationship between all the morphologic and mechanical parameters and age was analyzed by a linear regression and the Pearson's product–moment correlation coefficient in case of normal distribution. For nonnormal data distribution, a Spearman's rank test was used to analyze the association of morphologic and mechanical results. Agreement between the methods described for the elastic modulus measurement was assessed by the analysis of variance and its F test. The Bland-Altman method was used for graphically assessing the agreement.

Results

All MR examinations were correctly post-processed. The results of the morphologic analysis are shown in Table 1, with the values stratified by sex. Sex had a statistically significant influence on the bone volume-to-total volume ratio (p = 0.003) and trabecular thickness (p = 0.02) parameters, both greater in men (mean ± standard error of the mean [SEM] 0.24 ± 0.01 vs 0.21 ± 0.01 for bone volume-to-total volume ratio; 198.49 ± 3.19 μm vs 190.35 ± 0.95 μm for trabecular thickness) but only a tendency on trabecular separation (p = 0.06) (greater in women: 886.90 ± 24.61 μm vs 816.52 ± 26.46 μm) and trabecular number (p = 0.06) (greater in men: 1.22 ± 0.04 $10^{-3} \cdot \mu m^{-1}$ vs 1.10 ± 0.04

$10^{-3} \cdot \mu m^{-1}$). On the contrary, age had no statistically significant influence in any morphologic parameter (bone volume-to-total volume ratio, $r = -0.24$, $p = 0.13$; trabecular thickness, $r = -0.03$, $p = 0.88$; trabecular separation, $r = 0.12$, $p = 0.47$; and trabecular number, $r = -0.23$, $p = 0.16$) for male or for female healthy subjects (bone volume-to-total volume ratio, $r = -0.18$, $p = 0.46$ and $r = -0.13$, $p = 0.57$; trabecular thickness, $r = 0.09$, $p = 0.72$ and $r = 0.20$, $p = 0.38$; trabecular separation, $r = -0.22$, $p = 0.37$ and $r = 0.16$, $p = 0.50$; trabecular number, $r = -0.20$, $p = 0.41$ and $r = -0.15$, $p = 0.52$; male and female, respectively).

Significant differences were found between male and female subjects for the results of apparent elastic modulus ($p = 0.01$), with lower values in women, as can be observed in Table 1. There was no significant age influence ($r = -0.18$, $p = 0.26$).

A statistically significant relationship was found between the elastic modulus and the square of the bone volume-to-total volume ratio calculation ($r = 0.968$, $p < 0.001$), reflecting the high linear function between mechanical and structural parameters.

The volume of analyzed bone had an influence on the elastic results. Although the statistically significant difference between male and female results for apparent elastic modulus calculated in the small volume of interest (VOI) ($p = 0.002$) was maintained, reliability of results was reduced, and a statistically significant difference ($p < 0.001$) between apparent elastic modulus results obtained for the large VOI and those obtained for the small VOI (189.84 ± 20.02 MPa vs 81.56 ± 16.86 MPa) was obtained. Furthermore, the use of small volumes for elasticity calculation provided a nonnormal distribution and gave no statistical correlation ($r = 0.185$, $p = 0.25$) with the square of the bone volume-to-total volume ratio parameter. The behavior of the relationship between elastic modules calculated from the two different volumes and square of the bone volume-to-total volume ratio is seen in Figure 4, in which a linear performance is shown for the large volume, whereas no goodness of fit is found in the small volume estimation. Differences between apparent elastic modulus results for the two different analyzed volumes become greater when the values of the elastic parameter grow, as can be seen in the Bland-Altman plot (Fig. 5).

Discussion

Osteoporosis is a bone disease characterized by mass density reduction and a deterioration of the trabecular bone microarchitecture, finally increasing the risk of fracture. Because these factors are quite relevant as biomarkers of disease, both BMD and structural properties of the cancellous bone should be considered in the diagnosis and follow-up of this disorder.

In recent years, a morphologic analysis has been developed to test several trabecular bone physical properties such as the trabeculae dimensions and bone volume percentage [10, 11]. It has been also recognized that an evaluation of the mechanical behavior of the complete trabecular structure helps in the characterization of some bone properties [12, 15]. Therefore, any study designed to evaluate osteoporosis should include a detailed characterization of the trabecular bone structure as well as the bone mechanical properties. Also, to our knowledge, the evaluation of the influence of reducing the volume of analyzed bone, and therefore the computational burden, in the calculation of bone elastic properties has not been performed previously.

Image processing algorithms applied to high-resolution images are an important advance in the detection of new parameters acting as disease biomarkers. In our series, MR images were acquired from the distal metaphysis of the radius with a high spatial resolution, achieved in vivo with isotropic voxels of 180 μm. This small voxel size enables the development of a 3D model, allowing the characterization of the trabecular bone properties as new biomarkers of disease. Advanced image processing techniques, with segmentation, filtering, interpolation, and binarization of the trabecular bone region, were applied slice by slice to prepare the data for the 3D analysis.

Sex, but not age, has a clear influence on the morphologic bone parameters calculated from the trabecular 3D structure. Therefore, normal values of these parameters have to be stratified by sex. Variability of the obtained morphologic parameters also may be influenced by the acquisition and image processing techniques. In our study, the obtained morphologic parameters were in accordance with those previously published in other studies [12, 19]. However, some differences have to be mentioned. Our mean bone volume-to-total volume ratio was lower compared with Newitt et al. [12] (0.22 ± 0.04 vs 0.36 ± 0.05, respectively). Because those authors studied morphologic parameter results in a population of postmenopausal women and used a higher 3D slice partition thickness, these differences in spatial resolution and age distribution may be responsible for the disparity. Our mean trabecular thickness is in accordance with that obtained by Newitt et al. (0.19 ± 0.01 mm vs. 0.21 ± 0.02 mm) because the method of distance transform is characterized by its robustness in those cases having a higher spatial resolution than the typical dimensions of the tissue under study [10]. Our mean trabecular separation is also similar to that obtained in another study [19] for trabecular bone samples of the radius (0.85 ± 0.12 mm vs 0.75 ± 0.35 mm). Results obtained for trabecular number are also close to those published in that study (1.16 ± 0.19 mm^{-1} vs 0.96 ± 0.20 mm^{-1}).

Mechanical 3D analysis of complex structures by FE modeling has become a well-established method in engineering. The use of this tool has grown widely in recent years in bioengineering medical science, mainly because of the improvement of clinical imaging CT and MR scanners. The higher spatial resolution achieved with high-field 3-T MR scanners allows the development of 3D reconstructions of tissues with the possibility of simulation in defined conditions. Several studies [4, 12, 15] have shown the potential for application of the FE method in combination

TABLE 1: Mean Values of Morphologic and Elastic Results for the 40 Healthy Subjects Analyzed

Morphologic Parameter	Men ($n = 19$)	Women ($n = 21$)	Total ($n = 40$)
Bone volume-to-total volume ratio	0.24 ± 0.01	0.21 ± 0.01	0.22 ± 0.01
Trabecular thickness (μm)	198.49 ± 3.19	190.35 ± 0.95	194.22 ± 1.70
Trabecular separation (μm)	816.52 ± 26.46	886.90 ± 24.61	853.47 ± 18.66
Trabecular number ($10^{-3} \cdot \mu m^{-1}$)	1.22 ± 0.04	1.10 ± 0.04	1.16 ± 0.03
Apparent elastic modulus (MPa)	241.58 ± 28.07	143.02 ± 24.83	189.84 ± 20.02

Note—Data are expressed as mean ± standard error of the mean.

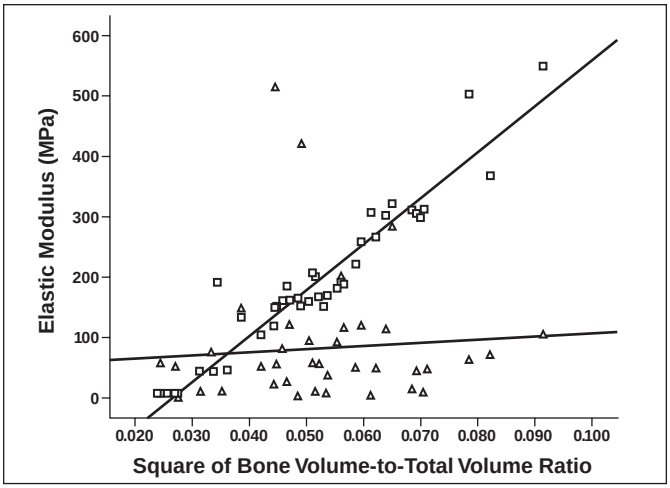

Fig. 4—On chart, different behaviors of correlation of apparent elastic modulus with square of bone volume-to-total volume ratio fraction parameter can be observed depending on analyzed volume of interest (VOI). Small VOI samples present no relationship of dependence with square of bone volume-to-total volume ratio fraction parameter. Large VOI samples have linear behavior and high correlation between apparent elastic modulus and square of bone volume-to-total volume ratio. □ = large VOI, △ = small VOI.

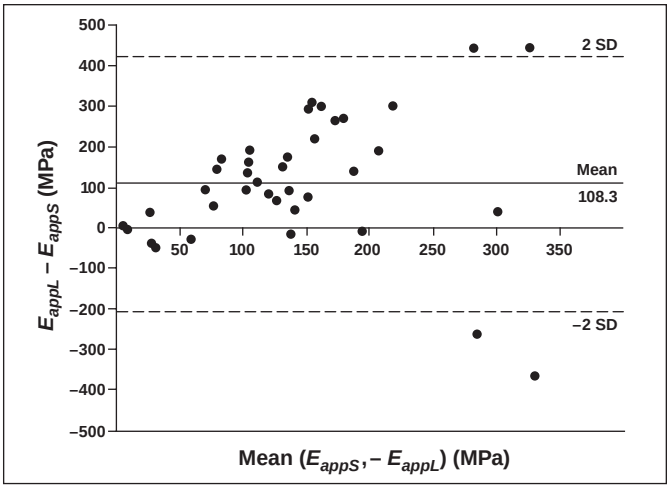

Fig. 5—Bland-Altman plot shows results of apparent elastic modulus for small volume (E_{appS}) and large volume (E_{appL}) analyzed.

with image processing techniques and voxel-based FE meshes to test the elasticity and quality of the trabecular bone.

In our study, simulated mechanical tests were applied to the in vivo trabecular bone reconstructions using the FE method with voxel-meshed structures. More accurate mechanical simulations are achieved by using a direct conversion from the voxels of the 3D reconstruction to the brick hexahedron elements of the FE model. Sex showed a significant influence on apparent elastic modulus results; Young's modulus results were greater in men, in accordance with our expectations [20].

We found that the mean elastic modulus obtained in our series was lower than the value obtained by Newitt et al. [12] for uniaxial compression (189.84 ± 126.62 MPa vs. 2,050 ± 590 MPa, respectively). Although the mechanical analysis presented by Newitt et al. is very similar to the one in this study, the methodology in our study presented some differences in acquisition technique regarding main magnetic field intensity (3 T vs 1.5 T), contrast sequence parameters (56/5 and flip angle, 25° vs 29/5.6 and flip angle, 30°), slice thickness (180 μm vs 500 μm), and image postprocessing (a subvoxel processing algorithm was developed in our study). Müller and Rüegsegger [21] obtained a compressive elastic modulus of the cancellous bone of the radius of 564 MPa using high-resolution CT with a slice thickness of 480 μm and the application of the FE method by tetrahedrons. Therefore, use of different acquisition techniques, image spatial resolution, and processing methods clearly influences the standardization of the apparent elastic modulus values.

When comparing in vivo relationships between elastic and morphology results, a high correlation for both sexes between elastic modulus (mechanical parameter) and the square of bone volume-to-total volume ratio (structural parameter) was found, agreeing with ex vivo tests in the relationship between apparent elastic modulus and bone volume-to-total volume ratio [17, 18]. This behavior agrees with the theory [22, 23] of the existence of a strong relationship between the elastic modulus and the square of porosity of a material in the elastic regime. This observed exponential dependence for the compressive modulus takes the form

$$\frac{E}{E_b} = C \cdot (BV / TV)^2$$

where E_b is the elastic modulus of the bulk (compact bone), which has been set to 10 GPa. From the results, a predicted value of C = 0.75 is obtained, giving the linear relationship between the square of bone volume-to-total volume ratio (BV/TV) and the apparent elastic modulus.

The main problems in the application of the FE method to trabecular bone meshes come from the high computational cost that composes the calculus of the solution of the linear system of equations (24 equations per voxel). To minimize the computational burden, a representative VOI may be chosen as small as possible if it provides reliable results. However, we have shown that the value of the results diminishes as the restricted volume dimensions decrease.

In our study, we have tested two different cancellous bone segmented volumes to evaluate the variation and reliability of the results. We have found that the mechanical analysis results applied to the large sample volumes of trabecular bone better characterize its properties, with significant differences between male and female subjects for the apparent elastic modulus parameter. As expected, results for this parameter were greater in men [23].

Some bias should be mentioned. In comparing age distribution in both sex populations, the female group presented three subjects over 60 years old, possibly distorting the tendency to provide significance. To test if these outliers could influence our results for the female group, the mean values for all the structural and mechanical parameters were compared between this small (three subjects) subpopulation and the remaining 18 female subjects using a Student's t test. Means were not significantly different between these two groups (p = 0.68, apparent elastic modulus; p = 0.60, bone volume-to-total volume ratio; p = 0.89, trabecular thickness; p = 0.18, trabecular separation; p = 0.59, trabecular

number). Thus, it was decided not to exclude them from the study.

No relationship was found between age and any of the parameters studied. These unlinked results probably may be enhanced by the relative youth of the subjects in our study (38 ± 15 years) in comparison with older patients, who tend to have an increase of osteoclast resorption, especially in women after menopause because of estrogen reduction [17]. This needs further study with larger and more age-representative series.

In conclusion, using advanced analysis of high-resolution 3-T MR images, it is possible to achieve 3D models of trabecular bone. Computer-generated 3D models of the cancellous bone can be used to further characterize bone, simulating different mechanical and structural scenarios for studying values and relationships of the obtained characteristic trabecular bone parameters. We found that bone volume-to-total volume ratio, trabecular thickness, and the elastic modulus are parameters influenced by the MR acquisition technique, computer processing, and sex. On the contrary, trabecular separation and trabecular number are independent values. Age did not seem to significantly influence any parameter in the healthy subjects analyzed. A high relationship has been found between elastic modulus and bone volume-to-total volume ratio. This association is lost when reducing the volume under analysis, also diminishing the reliability of the results. The usefulness of these morphologic and mechanical parameters in osteoporosis needs further evaluation. Results of the parameters comparing large series of osteoporotic and healthy subjects of different ages should provide knowledge for the establishment of new biomarkers of disease; offer more information to the patient; and, in so doing, both improve patient care and place radiology as an advanced technology in the implementation of new methods of diagnosis.

References

1. Newitt DC, van Rietbergen B, Majumdar S. Processing and analysis of in vivo high-resolution MR images of trabecular bone for longitudinal studies: reproducibility of structural measures and micro-finite element analysis derived mechanical properties. *Osteoporos Int* 2002; 13:278–287
2. Carballido-Gamio J, Majumdar S. Clinical utility of microarchitecture measurements of trabecular bone. *Curr Osteoporos Rep* 2006; 4:64–70
3. Seeman E. Invited review: pathogenesis of osteoporosis. *J Appl Physiol* 2003; 95:2142–2151
4. Chevalier Y, Pahr D, Allmer H, Charlebois M, Zysset P. Validation of a voxel-based FE method for prediction of the uniaxial apparent modulus of human trabecular bone using macroscopic mechanical tests and nanoindentation. *J Biomech* 2007; 40:3333–3340
5. Freedman D, Zhang T. Active contours for tracking distributions. *IEEE Trans Image Process* 2004; 13:518–526
6. Xu C, Prince JL. Snakes, shapes and gradient vector flow. *IEEE Trans Image Process* 1998; 7:359–369
7. Vasilic B, Wehrli FW. A novel local thresholding algorithm for trabecular bone volume fraction mapping in the limited spatial resolution regime of in vivo MRI. *IEEE Trans Med Imaging* 2005; 24:1574–1585
8. Hwang SN, Wehrli FW. Subvoxel processing: a method for reducing partial volume blurring with application to in vivo MR images of trabecular bone. *Magn Reson Med* 2002; 47:948–957
9. Otsu N. A threshold selection method from gray-level histogram. *IEEE Trans Systems Man Cybernet* 1979; 9:82–86
10. Saha PK, Wehrli FW. Measurement of trabecular bone thickness in the limited resolution regime of in vivo MRI by fuzzy distance transform. *IEEE Trans Med Imaging* 2004; 23:53–62
11. Tamada T, Sone T, Jo Y, Imai S, Kajihara Y, Fukunaga M. Three-dimensional trabecular bone architecture of the lumbar spine in bone metastasis from prostate cancer: comparison with degenerative sclerosis. *Skeletal Radiol* 2005; 34:149–155
12. Newitt DC, Majumdar S, van Rietbergen B, et al. In vivo assessment of architecture and micro-finite element analysis derived indices of mechanical properties of trabecular bone in the radius. *Osteoporos Int* 2002; 13:6–17
13. Fung YC. *Biomechanics: mechanical properties of living tissues*, 2nd ed. New York, NY: Springer, 1993:500–518
14. Zienkiewicz OC, Taylor RL. *The finite element method*, vol. 1: *The basis*, 5th ed. New York, NY: McGraw-Hill, 1989:18–37
15. Hollister SJ, Fyhrie DP, Jepsen KJ, Goldstein SA. Application of homogenization theory to the study of trabecular bone mechanics. *J Biomech* 1991; 24:825–839
16. Hollister SJ, Kikuchi N. A comparison of homogenization theory and standard mechanics analyses for periodic porous composites. *Comp Mech* 1992; 10:73–95
17. Zysset PK. A review of morphology–elasticity relationships in human trabecular bone: theories and experiments. *J Biomech* 2003; 36:1469–1485
18. Pothuaud L, Van Rietbergen B, Mosekilde L, et al. Combination of topological parameters and bone volume fraction better predicts the mechanical properties of trabecular bone. *J Biomech* 2002; 35:1091–1099
19. Majumdar S, Genant HK, Grampp S, et al. Correlation of trabecular bone structure with age, bone mineral density, and osteoporotic status: in vivo studies in the distal radius using high resolution magnetic resonance imaging. *J Bone Miner Res* 1997; 12:111–118
20. Keaveny TM, Yeh OC. Architecture and trabecular bone: toward an improved understanding of the biomechanical effects of age, sex and osteoporosis. *J Musculoskelet Neuronal Interact* 2002; 2:205–208
21. Müller R, Rüegsegger P. Three-dimensional finite element modelling of non-invasively assessed trabecular bone structures. *Med Eng Phys* 1995; 17:126–133
22. Brígido Diego R, Más Estellés J, Sanz JA, García-Aznar JM, Salmerón Sánchez M. Polymer scaffolds with interconnected spherical pores and controlled architecture for tissue engineering: fabrication, mechanical properties and finite element modeling. *J Biomed Mater Res Part B: Appl Biomater* 2007; 81B:448–455
23. Gibson LJ, Ashby M. The mechanics of foam: basic results. In: Clarke DR, Suresh S, Ward IM, eds. *Cellular solids: structure and properties.* Cambridge solid-state science series. New York, NY: Cambridge University Press, 2001:175–234